CHAPTER 4

OPTIMAL CVR: CENTRALIZED VOLT/VAR OPTIMIZATION

4.1 Introduction

The VVO is one of the featured functions of ADMS that have drawn more attention to utilities for optimal utilization of network control and assets in the distribution grid. It can perform various tasks such as CVR, loss reduction, voltage flattening and power factor correction [63],[13]. For peak load reduction, CVR approach is quite useful; therefore, DNOs are also preferring this method. Though, implementation of CVR with /or without DER through open-loop VVC schemes is an easier way but possesses certain inherent limitations of its adoption when changes occur in network configuration, power generation and demands [32]. On the other side, the closed-loop VVO schemes provide the superior action of VVC with higher energy savings through optimal operations of network assets and control setpoints. In literature, Various optimization algorithms have been used to solve the VVO problem, as explained in earlier *chapter 1* in the literature review section. Other researchers also have studied VVO related works such as an investigation on the loss of life estimation of distribution transformer through VVO method reported in [19], and a bi-level VVO approach has been introduced in [20] to coordinate the smart inverter dispatch and VVC devices simultaneously.

On the other hand, distributed energy storage (DES), especially Community Energy Storage (CES) is also drawing attention due to its inherent benefits such as peak load management, demand balancing and voltage regulation in distribution network operations [6], [115]–[120]. Moreover, the need of balancing the electricity consumption and energy system has also paved the way for CES installation tremendously [117]. The role of CES for shifting the load demand and energy surplus in real-time framework has

been investigated in [121]. The performance and cost benefits analysis with CES has been carried out in [118] considering the time shift impact of solar PV power generations. Optimal allocation and design of multiple CES system in ADN for economic assessment has been done in [122], [123]. The problem of rise in neutral voltage due to the unbalanced allocation of solar power and loads has been mitigated with CES as discussed in [124]. A coordinated control scheme for voltage regulation in distribution network via DES system has been studied in [125] . However, the above studies have not been explored the impact of CVR with DES. The study reported in [126], [127] reveals that the significant power saving can be achieved in the presence of CES in VVO solution. The studies reveal that lack of coordination between the network control such as CVR and asset controls at the energy storage can lead to detrimental effects for grid operations. In order to address this issue, a properly coordinated control scheme is required to integrate both CVR and CES operations simultaneously. Besides, the limited work has been reported in the literature to utilize the CES for maximizing the CVR benefits.

Therefore, this chapter introduces a centralized VVO driven optimal CVR methodology considering the impact of CES for ADNs.

4.2 Centralized Volt/VAR Optimization

A closed-loop framework for smart grid-enabled CVR has been shown in Figure 4.1. The main components of this framework are smart VVO engine located at the control center, VVC field devices (Distribution Transformer with OLTC, AVR, VAR inverters and CB), loads and measurement devices and AMI system. The framework is called closed-loop because it regularly monitors the measurements and sends the control signals to field devices through SCADA with the advanced communication system.

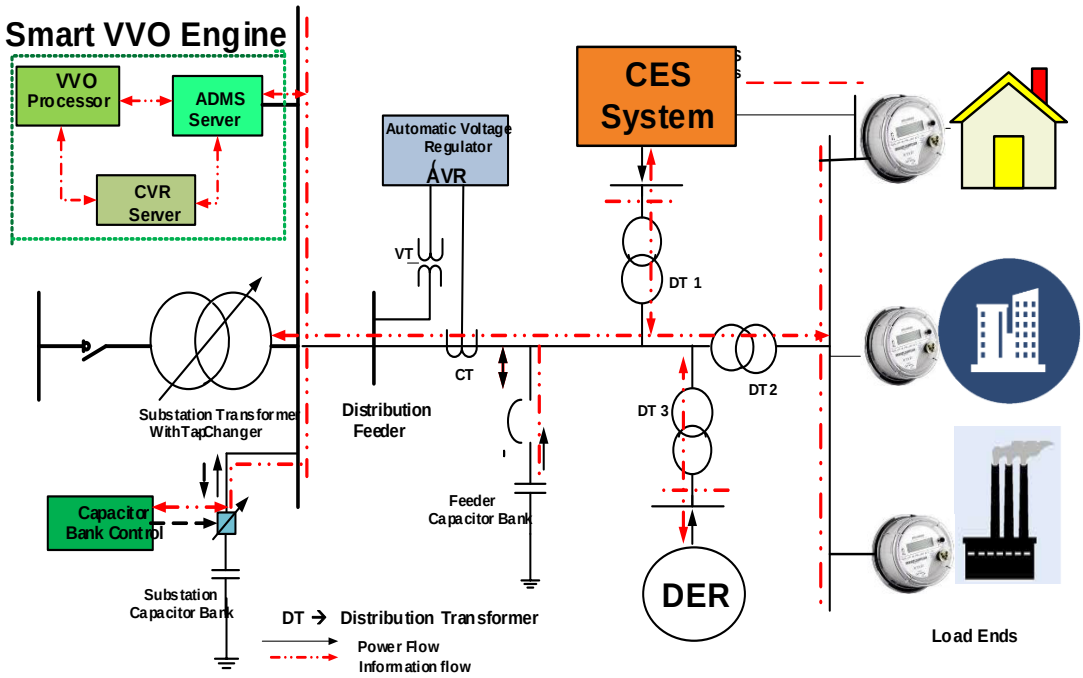

Figure 4.1: Proposed closed-loop VVO based smart grid-enabled CVR

4.2.1 VVO based CVR

In this work, a VVO driven CVR method has been proposed for smart grid operations. It consists of a VVO processor and CVR server assisted through ADMS as shown in Figure 4.1. The main task of VVO processor is to provide the optimal control set points according to desired objectives. The role of CVR server is to provide the CVR settings (such as voltage and time duration) to VVO processor. The control center operator has flexibility to choose different tasks such as loss reduction, voltage flattening, network reconfiguration and CVR. The numerous works have been reported in the literature with the objective of losses reduction, voltage flattening, and network reconfiguration. In this study, the main objective of VVO engine is to enable the CVR. In order to achieve this, the CVR server helps the VVO processor to determine the optimal VVC device settings. The minimization of the total power consumption satisfying the system constraints has been considered as an objective function. In order to achieve this objective, VVO

processor optimizes the voltage and VAR settings of VVC devices in such a manner that the feeder voltage profile remains within the regulatory range.

4.2.2 Estimation of CVR savings

Generally, CVR savings are estimated in terms of technical and economic value. The power and energy saved to add the technical value and cost savings referred as economic gain. Therefore, the employed CVR scheme has been assessed in terms of reduction in the amount of peak power, saving in energy, cost and CVR factors.

4.2.2.1 Estimation of Power, Energy and Cost Saving:

The total peak active power demand reduction, ΔP_{demand}, energy savings, ΔE_{saving}, and cost savings, ΔC_{saving} have been estimated using equations (4.1)- (4.3) respectively.

$$\Delta P_{demand} = P_{demand}^{No-CVR} - P_{demand}^{CVR},\ \%\Delta P_{demand} = \left(\frac{\Delta P_{demand}}{P_{demand}^{No-CVR}}\right)\times 100 \tag{4.1}$$

$$\Delta E_{saving} = E_{demand}^{No-CVR} - E_{demand}^{CVR},\ \%\Delta E_{saving} = \left(\frac{\Delta E_{saving}}{E_{demand}^{No-CVR}}\right)\times 100 \tag{4.2}$$

$$\Delta C_{saving} = C_{\cos t}^{No-CVR} - C_{\cos t}^{CVR},\ \%\Delta C_{saving} = \left(\frac{\Delta C_{saving}}{C_{\cos t}^{No-CVR}}\right)\times 100 \tag{4.3}$$

where P_{demand}^{No-CVR} E_{demand}^{No-CVR} and $C_{\cos t}^{No-CVR}$ are the active power demand, energy demand and cost of power purchase (*Cpp*) respectively during No-CVR operation. However P_{demand}^{CVR}, E_{demand}^{CVR} and C_{cost}^{CVR} are the active power demand, energy demand and cost of power purchase respectively during CVR operation.

The cost of power purchased has been determined using the cost of energy and it has been expressed in equation (4.4) as function ($F_{C_{PP}}$).

$$F_{C_{PP}} = \sum_t^T [C_{Grid}(t) P_{demand}(t)] \tag{4.4}$$

The values of C_{cost}^{No-CVR} and C_{cost}^{CVR} have been determined using equations (4.5) and (4.6) for the time period T, as shown below:

$$C_{cost}^{No-CVR} = \sum_t^T [C_{Grid}(t) P_{demand}^{No-CVR}(t)] \quad (4.5)$$

$$C_{cost}^{CVR} = \sum_t^T [C_{Grid}(t) P_{demand}^{CVR}(t)] \quad (4.6)$$

where $C_{Grid}(t)$ is the grid electricity price at time t and $P_{demand}^{No-CVR}(t)$, $P_{losses}^{No-CVR}(t)$ are the load demand and losses at time t respectively during No-CVR operation. $P_{demand}^{CVR}(t)$ and $P_{losses}^{CVR}(t)$ are the load demand and losses at time t respectively during CVR operation.

4.2.2.2 Estimation of CVR factor

In order to check the effectiveness of CVR in technical terms, CVR factor has been calculated in terms of peak kW power (CVR_{fP}) and kWh energy (CVR_{fE}). From an economic point of view, CVR factor has been calculated in terms of cost savings in purchased power. In this study, CVR factor is estimated in terms of peak active power reduction, energy savings and cost savings with respect to the percentage of voltage reduction as delineated under:

- *CVR factor in terms of active peak power demand (CVR_{fP}):* The CVR_{fP} (kW) is the ratio $\%\Delta P_{demand}$ to percentage voltage reduction (%ΔV).

$$CVR_{fP} = \frac{\%\Delta P_{demand}}{\%\Delta V},\ \%\Delta V = \left(\frac{V_{No\text{-}CVR} - V_{CVR}}{V_{No\text{-}CVR}} \right) \times 100 \quad (4.7)$$

where $V_{No\text{-}CVR}$ and V_{CVR} are node voltage during No-CVR (normal operation) and CVR operation respectively.

- *CVR factor in terms of energy savings (CVR_{fE}):* CVR_{fE} (KWh) is measured as the ratio of $\%\Delta E_{saving}$ to %ΔV.

$$CVR_{fE} = \left(\frac{\%\Delta E_{saving}}{\%\Delta V} \right) \quad (4.8)$$

- CVR factor in terms of economic (CVR_{fC}): CVR_{fC} (K$) is the ratio of %ΔCsaving to %ΔV.

$$CVR_{fC} = \left(\frac{\%\Delta C_{saving}}{\%\Delta V} \right) \tag{4.9}$$

4.3 Distributed Energy Storage

Application of energy storage systems in distribution grid are generally categories as utility-owned and customer-owned storage systems. Placing new storage systems and distributed energy resources near loads offer many potential applications. A customer location-based new storage system is generally referred to as a DES system [116], [119],[128]. One of the most popular examples of DES is a CES system nowadays. CES technologies are being accepted and deployed globally because of their salient benefits, such as active/reactive power support, load-demand balancing, frequency and voltage regulation, and ancillary services [5].

4.3.1 Community Energy Storage

CES is a defined as small DES system in the range of few kW to hundreds of kW that are connected to the secondary of the transformer feeding the power to a few residential /small commercial consumer loads with proper coordination [116], [119], [123]. The rated power capacity of CES units typically varies from 25 kW to 50 kW with the discharge time from one to three hours [5], [18]. The typical CES system and its control have been shown in Figure 4.2. The main components of CES system can be divided into following three main parts:

4.3.2.1 Smart Control and Management System

The three-layered intelligent control approach is best suited for the CES system. The first layer mainly deals with centrally controlling of the energy management system and the

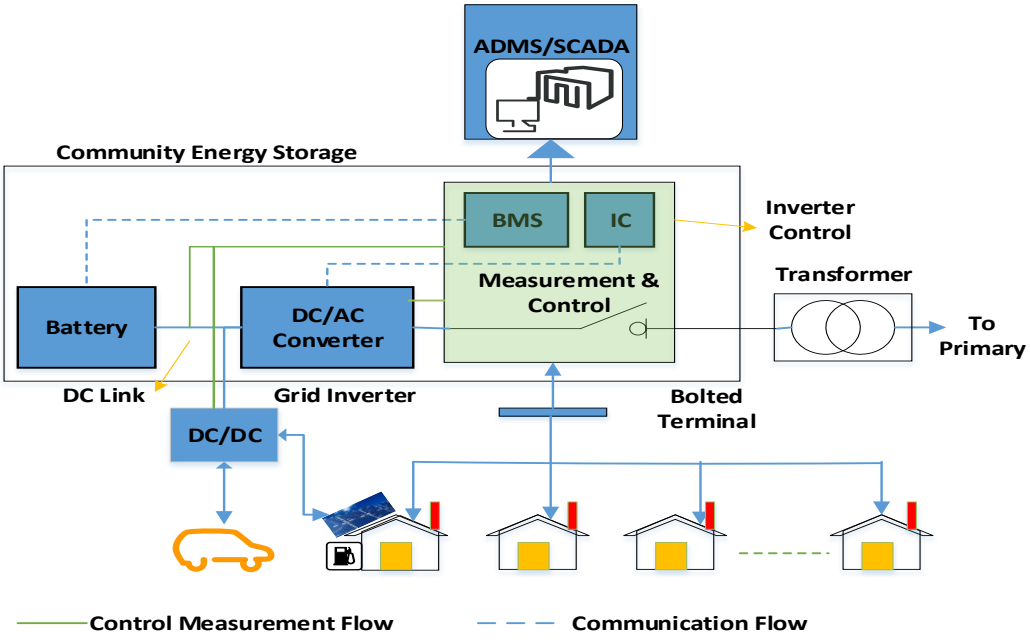

Figure 4.2: Schematic layout of CES system [127]

second is regional control for optimization at the substation transformer level, feeder and for a group of CES units. The third layer operates locally for controlling the CES unit at an individual inverter level at low voltage and islanding mode. CES management system which consists of a battery, inverter control and battery management system (BMS) connected to the Point of Connnection (POC) and ADMS/SCADA system. This POC is connected to the secondary side of the distribution transformer.

4.3.1.2 Power Conversion System (PCS):

The second part is the power conversion system having DC/AC and AC/DC converters through which battery is connected to POC and control blocks. PCS is a main part of the CES system because the whole power conversion process is executed with the help of PCS. The main part of PCS is a smart converter (which converts both AC to DC and DC to AC) combined with a smart inverter controller. Modern smart inverter having the facility to operate in four quadrants in bidirectional mode is deployed in CES system. With the use of these inverters, CES can provide both active and reactive power to the distribution grid or locally.

4.3.1.3 Communication System and Advanced Protection

The third part covers the measurements and communication system which monitors, measures the status of connected devices and sends/receives the control signals to ADMS through the advanced communication system. Generally, distributed energy management interface using a DNP based communication standard is preferred [116], [117]. The CES system is equipped with advanced protection devices such as isolators, DC modules, circuit breakers, Fuse and protection scheme which can clearly differentiate between the islanding conditions and abnormal conditions [116].

4.3.2 CES Control Strategy

The three-layered intelligent control approach is best suited for CES operation. The first layer deals with centrally controlling of the energy management system. Optimal control strategy at substation transformer level, feeder level, and a group of CES units is determined at the second layer and referred as the regional control layer. The local control of CES unit at an individual inverter level is performed at the third layer. Each layer can operate separately and/or combined with other layers. The present investigation focuses mainly on first and second layers for VVC and demand balancing at the substation feeder level. This can be achieved through controlling of CES system.

4.3.2.2 Charging/discharging control strategy of battery management system (BMS):

The control strategy of BMS operates in three states, such as charging, discharging and idle, as shown in Figure 4.3. The strategy begins with identifying the substation loading in three categories such as low, normal and high as recognized by the operator. During the low/off loading, CES system consumes power from the network, i.e. CES units operate in the charging state. Prior to operation in the charging state, it is to be ensured that the kWh stored value ($kWh_{CES,T}^{stored}$) is less than rated kWh capacity (kWh_{CES}^{rated}). Then after, it is to be ensured that the current State of Charge (SOC^T) should be below the upper

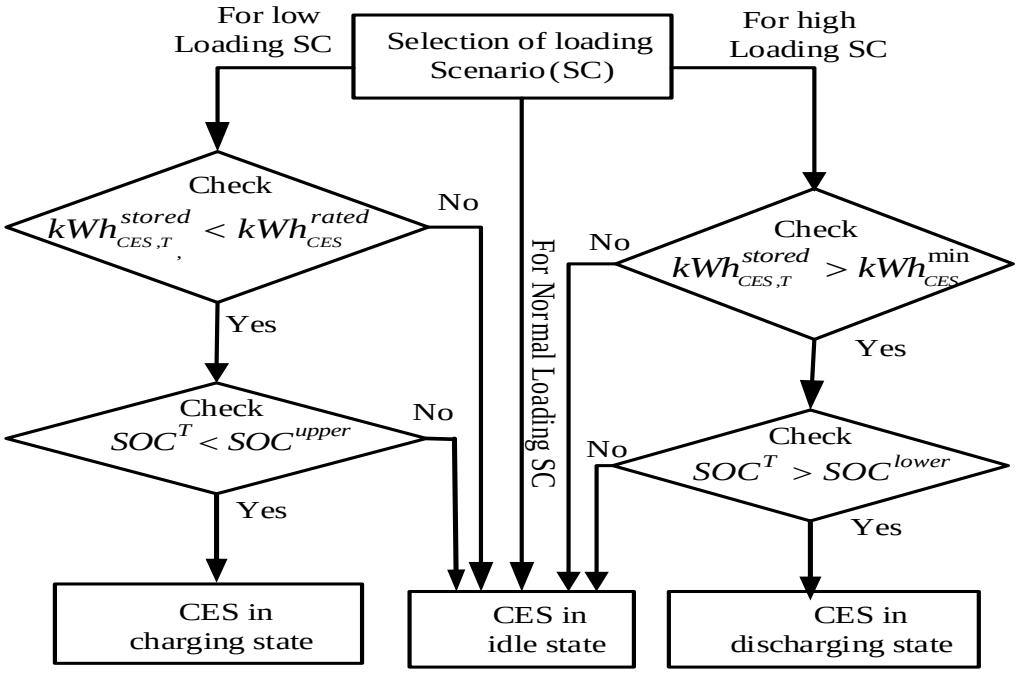

Figure 4.3 Charging /discharging control strategy of BMS

limit of SOC (SOC^{upper}). During the high loading period, CES system operates in the discharge state. However, a higher value of $kWh_{CES,T}^{stored}$ than the minimum specified kWh capacity ($kWh_{CES,T}^{stored}$) of the CES should be ensured before an operation in a discharged state. The (SOC^{T}) should be continuously monitored and it should be maintained above the specified lower limit of SOC (SOC^{lower}). Moreover, during normal loading hours, CES remains in the idle state, i.e., it neither charge nor discharge the CES unit. The SOC of battery at time T is defined by equation (14).

$$SOC^{T} = \left(\frac{kWh_{CES,T}^{stored}}{kWh_{CES}^{rated}} \right) \tag{4.10}$$

4.3.2.3 CES power flow control for Unbalanced Network:

The power flow control strategy at POC of CES has been depicted in Figure 4.4. The unbalance distribution networks have uneven loading in each phase of the feeder. The highest and lowest loading phase at POC of the CES and network is identified before the power flow control is applied.

During charging state, CES system is connected to the lowest loading phase. It consumes power from the grid during the charging state. The CES power output (CES^{Pout}) is equal to CES^{Pout} and it acts as a load. However, during discharging state, CES system is connected to the highest loading phase and it injects the power into the grid. The CES power output is negative and the CES acts as power source. Moreover, in the idle state, CES is disconnected from the network. It is further to be mentioned that the control strategy described in *subsection 4.3.3.2* is applied without any modification.

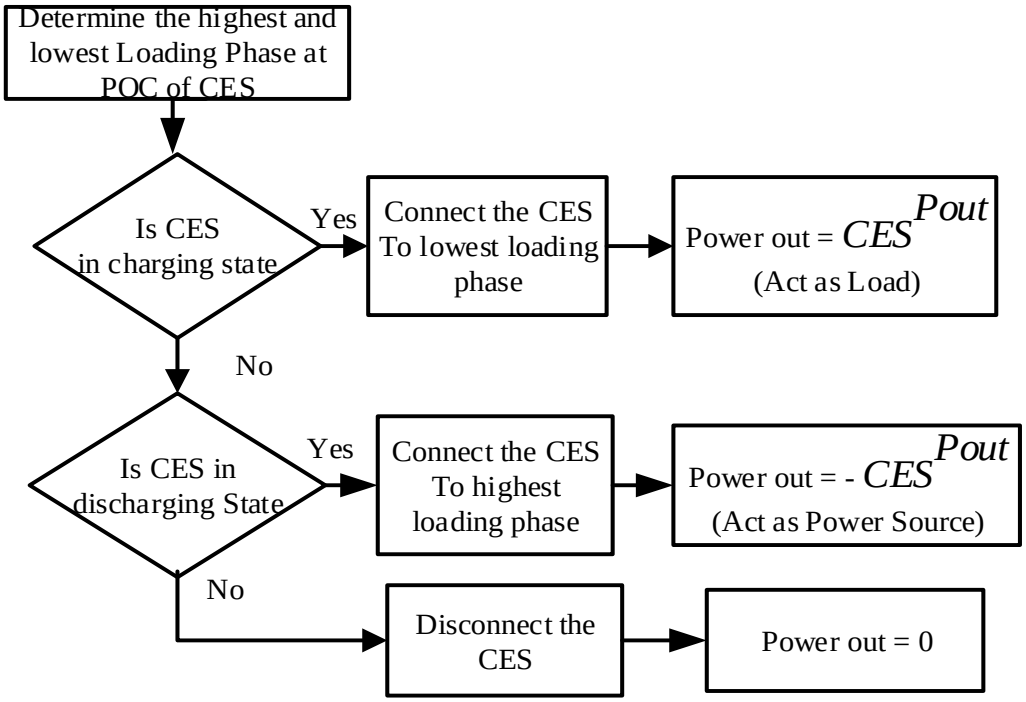

Figure 4.4 CES power flow control

4.4 Problem Formulation and Solution Method

The basic goal of this study is towards, the development of VVO engine for CVR, to achieve higher energy efficiency and peak shaving in the presence of DER and CES. In this section, the problem formulation and solution method for VVO is delineated.

4.4.1 Problem Formulation

In order to deploy the CVR, a VVO engine-based method has been adopted in this work. The VVO engine minimizes the total power demand from the substation allowing

variations in tap positions of OLTC, AVRs and CBs switching. The objective function and constraints are delineated as under.

4.4.1.1 VVO Objective Function:

Total active power demand is the summation of total active power loads ($P_{Total\ Load}$) and active power loss ($P_{Total\ Loss}$) of the active distribution system; thus, the objective function can be written as:

$$Objective\ \ function = \text{minimize}\left(P_{Sub}^{Demand}\right) \tag{4.11}$$

$$P_{Sub}^{Demand} = \sum\left(P_{Total\ Load} + P_{Total\ Loss}\right) \tag{4.12}$$

$$P_{Total\ Load} = \sum_{k=1}^{Nl}\sum_{\phi\in A,B,C} P_{L,k}(V_k)^{\phi} \tag{4.13}$$

$$P_{Total\ Losses} = \sum\left(P_{loss}^{lines} + P_{loss}^{cables} + P_{loss}^{txf} + P_{loss}^{inv,CES}\right) \tag{4.14}$$

here $P_{Total\ Losses}$ is the total active power losses and $P_{Total\ Load}$ is the total active power load of all phases and $P_{L,k}(V_k)$ is the load at *k*th node. Φ represents the phase A,B,C and Nl is the total load node number. $P_{Total\ Losses}$ are the total active power losses on lines (P_{loss}^{lines}), cables (P_{loss}^{cables}),inverter ($P_{loss}^{inv,CES}$) and transformers (P_{loss}^{txf}) as shown in (4.14). From equation (4.13), it can be observed that the real power demand at a node is dependent on its voltage. Further, it reveals that the demand would decrease with a decrease in voltage. Transformer core losses depend upon the voltage, whereas transformer winding and line losses mainly depend upon current flows. Therefore, total active power losses may decrease or increase with reduced voltage.

4.4.1.2 Decision Variable (X)

The taps of OLTC, AVRs and switching steps of capacitor banks are the main decision variables as shown below.

- tap position of OLTC (T_P^{OLTC})
- tap position of AVR (T_P^{AVR})
- CBs reactive power ($Q_{i,cb}^t$)

$$X = \left[T_P^{OLTC}, T_P^{AVR}, Q_{i,cb}^t \right] \tag{4.15}$$

4.4.1.3 System Constraints

The scheduled VVO problem is subjected to the following constraints:

- *Power Balance Constraints:* The constraints dealing with active and reactive power balance constraints are expressed using (4.16) and (4.17) respectively.

$$P_{grid} + P_{DER} \pm P_{CES} - P_{Total\ Load} = V_h \sum V_k (G_{hk} cos\theta_{hk} + B_{hk} \sin\theta_{hk}) \tag{4.16}$$

$$Q_{grid} + Q_{CES} + Q_{cb} + Q_{CES} - Q_{load} = V_h \sum V_h (G_{hk} cos\theta_{hk} - B_{hk} \sin\theta_{hk}) \tag{4.17}$$

where P_{grid} Q_{grid} are the active and reactive power taken from the external grid respectively. P_{CES} , Q_{CES} denotes the active, reactive power of CES and Q_{load} , Q_{cb} are the total reactive power load and reactive power supplied by capacitor banks at time t. G_{hk} , B_{hk} and θ_{hk} represent the conductance, susceptance matrices and phase angle between nodes h and k respectively. The voltage profile at *k*th node is denoted by V_k .

- *Transformer/regulator tap constraints:* The tap range of OLTC transformers/AVR and tap position are given in (4.18) and (4.19) respectively.

$$0.9\text{pu} \le \text{Tap} \le 1.1\text{pu} \tag{4.18}$$

$$\text{Tap} = \left\{ 1 \pm \left(\frac{\Delta V_{tr}}{100} \right) \times T_P \right\} ,\ T_p \in \left\{ T_p^{\min}, ...0.....T_p^{\max} \right\} \tag{4.19}$$

where ΔV_{tr} is increment in voltage at each step and T_p is tap position. $T_p^{\min}$ and $T_p^{\max}$ are the minimum and maximum tap values.

- *CB constraints:* Reactive power supply by CB at each switching operation is determined by equation (1.12) and detailed explained in *chapter 1*.
- *Voltage constraints:* The voltage profile of the distribution feeder should be maintained within limits, as shown in equation (3.13) and explained in *chapter 3*.
- *DER operation Constraints:* The equation (30) shows the active power (PDER) generated by DER is equal to the forecasted value (PfDER). Equation (4.21) represents the reactive power (QDER) generated using power factor angle (_ϕ_{DER}) of DER. Equation (4.22) represents the DER capacity (S_{DER}) constraint.

$$P_{DER} = P_{DER}^{f} \tag{4.20}$$

$$Q_{DER} = P_{DER} \tan \phi_{DER} \tag{4.21}$$

$$S_{DER} \leq \sqrt{\left(P_{DER}\right)^2 + \left(Q_{DER}\right)^2} \tag{4.22}$$

- *CES Constraints:* The operation constraints of CES are shown in equations (4.23) to (4.27).

CES voltage limit:

$$V_{CES}^{\min} \leq V_{CES} \leq V_{CES}^{\max} \tag{4.23}$$

where V_{CES} is the CES terminal voltage and $V_{CES}^{\max}$ $V_{CES}^{\min}$ denotes the maximum and minimum ranges of $V_{CES,}$ respectively.

CES power limit:

Active and reactive power ($P_{CES,T}$ and $Q_{CES,T}$) limit at time T should be less than or equal to its rated value as shown in equations (4.23) and (4.24) respectively. Total power supplied/absorbed by CES system governed by the (4.25).

$$P_{CES,T} \leq P_{CES}^{rated} \tag{4.23}$$

$$Q_{CES,T} \leq Q_{CES}^{rated} \tag{4.24}$$

$$\left(\sqrt{P_{CES,T}^2 + Q_{CES,T}^2}\right) \leq \left|S_{CES,inv}\right| \tag{4.25}$$

where, $P_{CES}^{\max}$ & $P_{CES}^{\min}$ is maximum and minimum value of P_{CES} and $S_{CES,inv}$ is the CES inverter KVA capacity.

CES capacity limit:

$$kWh_{CES}^{\min} < kWh_{CES,T}^{stored} < kWh_{CES}^{rated} \tag{4.26}$$

CES battery SOC limit:

The SOC of CES battery is determined by (4.10) and it should follow the relation (4.27) at T time operation.

$$SOC^{lower} < SOC^{T} < SOC^{upper} \tag{4.27}$$

4.4.2 Proposed VVO Solution using DGSA

The VVO problem has been solved through a Discrete Gravitational Search Algorithm (DGSA) that bears interest in highly complex optimization problems regarding faster convergence and real-time applications [129]. It has been reported to be an efficient method for solving different optimization problems in power systems [130], [131]. The optimization of the static VAR compensator parameters has been achieved through GSA for reactive power compensation in real time application by authors of [132]. Enhanced GSA has been employed for feeder reconfiguration, losses and operational cost minimization in distribution network [130]. In [131], binary GSA has been utilized for optimal cost and observability of wide area measurement Thus, GSA has been found to be suitable method for optimization of parameters of changing operational scenario and real time applications. The present optimization problem deals with discrete control

variables (tap positions and capacitor switching steps). Therefore, the basic concept of GSA has been extended to incorporate discrete search space.

4.4.2.1 Overview of Gravitational Search Algorithm (GSA)

A GSA driven optimization approach is proposed to solve the VVO problem expressed by equations (4.11) through (4.27). Esmat Rashedi et al., [129] introduced a new intelligent search technique called GSA, which is based on gravitational law and concept of mass interactions. In this technique, agents are collection of masses which interact with each other based on the Newton gravitational law and the laws of motion. Consider a system with *n* number of agents with *d* dimensions, in which the position of the i^{th} agent is defined as:

$$X_i = (x_i^1, x_i^2, x_i^3 .....x_i^n) \tag{4.28}$$

At a particular time'*t*,' the force ($F_{ij}^d(t)$) acting on 'i^{th}' mass from 'j^{th}' mass would be,

$$F_{ij}^d(t) = G(t)\frac{M_{pi}(t) \times M_{aj}(t)}{R_{ij}(t) + \xi}(x_j^d(t) - x_i^d(t)) \tag{4.29}$$

At particular time't,' $G(t)$ is the gravitational constant $M_{pi}(t)$ is the passive gravitational mass of i^{th} agent and $M_{aj}(t)$ is the active gravitational mass of j^{th} agent. $R_{ij}(t)$ is the Euclidian distance between the i^{th} and j^{th} agent. ξ is a small constant. The total force ($F_i^d(t)$) acts on an i^{th}agent in d^{th} dimension, and its acceleration ($a_i^d(t)$) from other agents is expressed in (4.30) and (4.31) respectively.

$$F_i^d(t) = \sum_{j=1, j\neq i}^{n} rand_j F_{ij}^d(t) \tag{4.30}$$

$$a_i^d(t) = \frac{F_i^d(t)}{M_{ii}(t)} \tag{4.31}$$

where, *rand* is a random number in the interval [0, 1], M_{ii} is the inertial mass of i^{th} agent.

Velocity ($v_i^d(t)$) and position ($x_i^d(t)$) of the i^{th} agent in the d dimension is updated as follows:

$$v_i^d(t+1) = rand_i \times v_i^d(t) + a_i^d(t) \tag{4.32}$$

$$x_i^d(t+1) = x_i^d(t) + v_i^d(t+1) \tag{4.33}$$

And the masses of each agent are updated by

$$m_i(t) = \frac{fit_i(t) - worst(t)}{best(t) - worst(t)}, \quad M_i(t) = \frac{m_i(t)}{\sum_{j=1}^{n} m_j(t)} \tag{4.34}$$

best = Minimum ($fit_i(t)$) *and worst =Maximum*($fit_i(t)$)

where, *best* and *worst* both depend upon the objective function.

Gravitational constant (G) can be obtained by (4.35):

$$G(t) = G_0 e^{-\alpha \frac{t}{Tr}} \tag{4.35}$$

where G_0, α are the constant parameters and *Tr* is total number of iterations.

4.4.2.2 Discrete GSA

In general, GSA has been mainly used to solve the continuous optimization problems. For solving the discrete optimization problems, the GSA cannot be applied directly due to its internal coding structure. The present VVO problem is an example of the discrete optimization problem. Therefore, following modifications have been done in GSA code before solving the present optimization problem.

- Integer random initialization has been carried out by selecting the nearest integer value of the variables.
- During computation, the new position of the variables is also rounded to the nearest integer value as expressed by equation (4.36).

$$x_i^{d'}(t) = round(x_i^d(t)) \quad (4.36)$$

where, $x_i^{d'}(t)$ is modified d^{th} position value of the i^{th} agent.

4.5 Implementation of VVC Scheme

In this section, the implementation of CVR with traditional method and proposed smart grid enabled CVR through VVO method have been described. The modelling of distribution network, CES system and implementation of CVR methods have been done in OpenDSS and MATLAB platform interfaced through component object model. Figure 4.5 shows the interacting framework of OpenDSS and MATLAB platforms.

4.5.1 Traditional CVR

Traditionally, LDC scheme are deployed for voltage reduction. Figure 4.6 (a) shows the flowchart of the implementation of CVR applying LDC. The regulated /EOL voltage is fixed in the lower half range (120-114V) of the service voltage. The control action is determined through LDC algorithm.

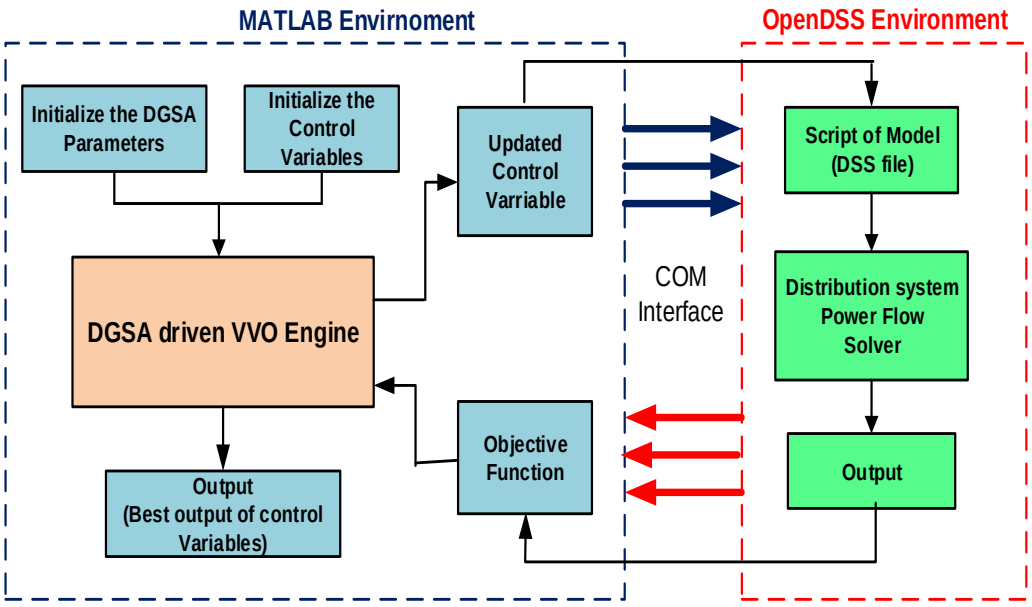

Figure 4.5 Interacting framework of OpenDSS and MATLAB platforms.

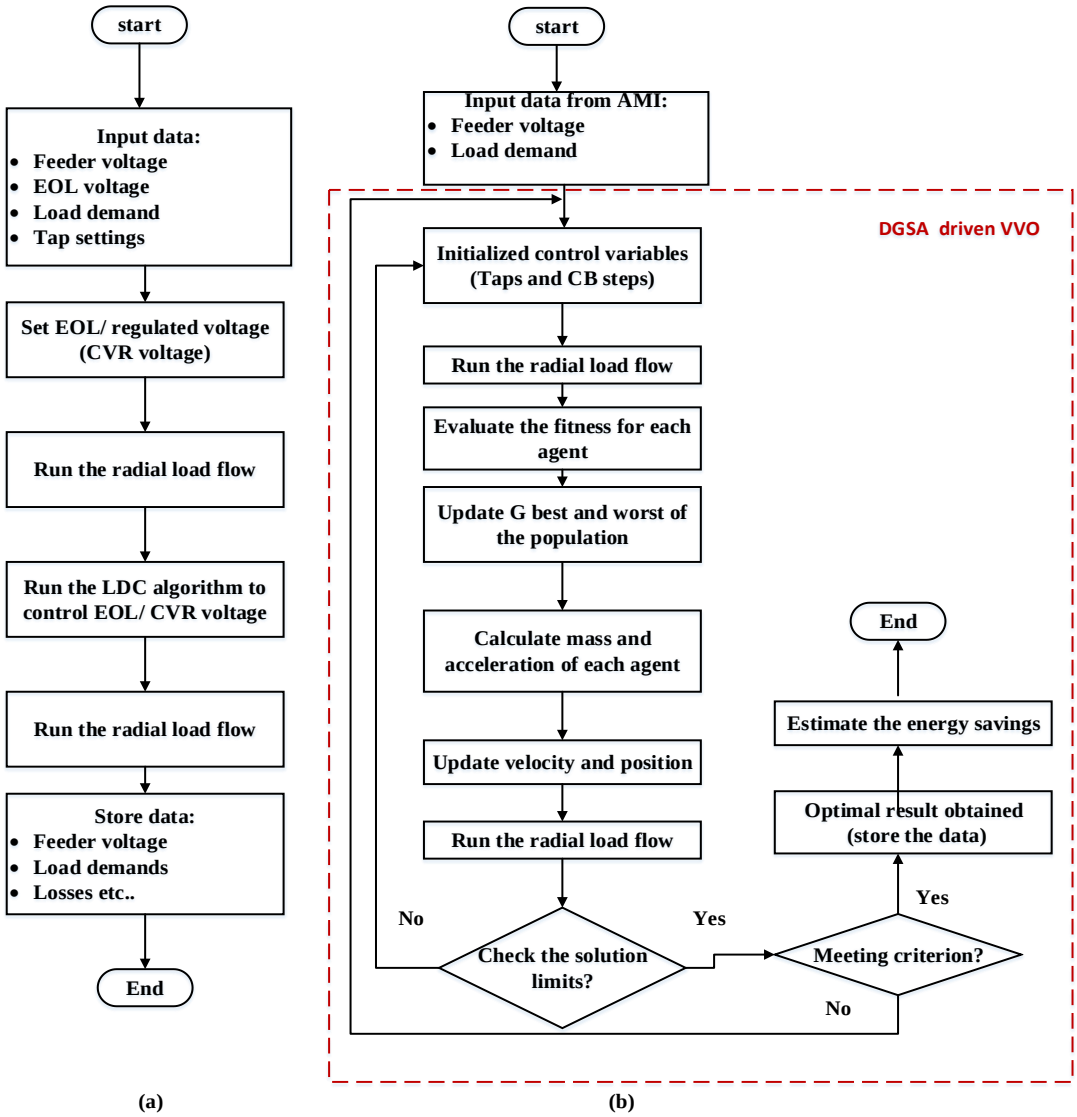

Figure 4.6 Flowchart of CVR methods implementation (a) Traditional CVR Approach (b) SG enabled VVO based CVR

4.5.2 Smart Grid (SG) enabled CVR

The proposed smart grid enabled CVR has been implemented through VVO approach. The DGSA driven VVO has been utilized in this study. The VVO method implementation, estimation of energy savings and CVR factor has been carried out mainly in following two stages:

- In the first stage, deployment and execution of VVO solution is performed. The parameters of VVC devices such as taps, steps of CBs, active & reactive power flows

through CES are obtained through VVO engine. The VVO engine has been developed in MATLAB environment with DGSA driven optimization approach.

- In the second stage, energy savings and CVR factor are estimated using the optimal results obtained in first stage.

The dimension of agents has been divided into various sets such as tap positions of OLTC, AVRs and CB switching. The maximum number of iterations (*Tr*) has been taken as stopping criteria. Step wise procedure of proposed VVO solution is delineated in *algorithm 1* as under:

Algorithm 1 VVC Parameters optimization using DGSA	
1	**Input:** Feed the distribution network data {loads, lines, VVC devices and CES data
2	**Input:** GSA parameters and control varriable limit
3	Set the multiplier of active and reactive power load
4	Enable the CES control stretegy as explained in *subsection 4.3.2* (If CES is present/participating)
5	Divide the dimension of agent among control variables (as tap positions of OLTC, AVRs, and switching steps for CBs & CES)
6	Set the stopping criteria (maximum number of iterations)
7	Initialize population and speed of all the particles in MATLAB and perform load flow analysis in OpenDSS.
8	Evaluate the value of fitness function expressed by equation (4.11) for each agent in MATLAB.
9	Find best and worst among all the agents
10	Calculate force and masses on each agent using equations (4.29) and (4.34) respectively.
11	Calculate acceleration and velocity of each agent using equations (4.31) and (4.32) respectively.
12	Update velocity and position of each agent.
13	Check the stopping criteria if yes then go to *step 14* else move to next iteration.
14	Adopt the settings of VVC devices corresponding best solution
15	**Output:** Estimate energy saving and CVR factor using equations (2.1) and (2.2) respectively.

Implementation of above-described algorithms using OpenDSS and MATLAB has been further explained using a flow chart given in Figure 4.6 (b).

4.6 Case Study

The proposed VVO based CVR Scheme has been validated using in two scenarios as:

- Scenario-1: Demand reduction during fully loading hours
- Scenario-2: Energy saving and demand management during varying load hours

4.6.1 Test System Discription

The proposed CVR method has been validated on modified IEEE 123 node distribution test system as shown in Figure 4.7(a) [114]. It is named modified system due to addition of DER, a CES system and change in load model for demonstration purpose. Voltage dependent constant impedance current power (ZIP) load model has been considered in this study and detailed description can be seen in *chapter 1* under subsection *1.4.3*. The values of ZIP coefficients under various loading types with respect to nodes have been written Table A.2 in Appendix A. The loads in test system contain primary spot and distributed loads at primary. These loads are represented as lumped loads [18]. The model of this system stops at the primary nodes, therefore the secondary distribution system (SDS) configuration connect to CES at POC node has been modelled and shown in Figure 4.7 (b). For example, the kVA of the spot load at 65 is calculated as $\sqrt{(150)^2 + (100)^2}$ = 180 kVA; therefore, this primary node (node 65) can be replaced by a 180-kVA distribution transformer serving a SDS, to match the original spot load. In order to alter the CES connection with different phases during the charging/discharging mode of operation, a switch has been equipped with CES installation systems as shown in Figure 4.7(b).

In this chapter, the DERs are classified as non-renewable and renewable power sources with unity power factor. In context of renewable source, two wind turbine-based power sources located at node 95 and 151 have been considered. The details of wind power modeling can be found in [133]. Ratings and parameters of VVC devices, DERs

and CES have been shown in Table 4.1, Table 4.2 and Table 4.3 respectively. The voltage increments at each step, ΔV_{tr} has been chosen as 0.625.

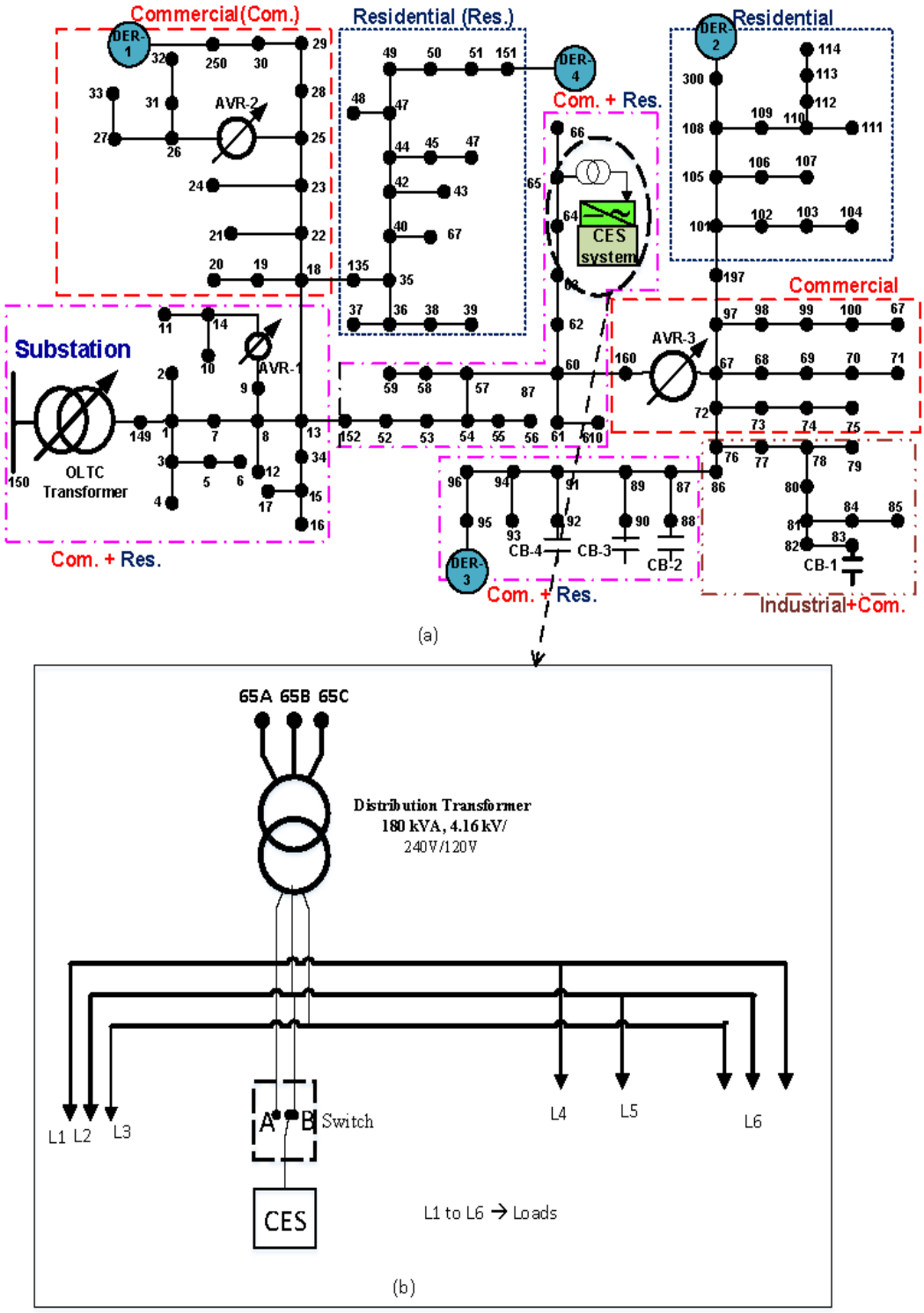

Figure 4.7: (a**)** Modified IEEE 123 node distribution test feeder
(b) Secondary distribution system (SDS) configuration connect to CES at POC node 65

Table-4.1. Ratings and Parameters of VVC devices

Device	**Phase /Connection**	**Location/ rating**		**Tap range / CB step** ($T_p^{\min}$,$T_p^{\max}$, $Sw_{cb}^{p,\max}$)
OLTC	3-Phase, Wye	150 - 149		+16 to -16
AVR-1	1- Phase (A)	9-14		+16 to -16
AVR-2	2- Phase (A, C)	25-26		+16 to -16
AVR-3	3- Phase	160-67		+16 to -16
CB-1(kVAR)	3- Phase	83	200/Phase	0-4
CB-2(kVAR)	1- Phase (A)	88	50/ Phase	0-1
CB-3(kVAR)	1- Phase (B)	90	50/ Phase	0-1
CB-4(kVAR)	1- Phase (C)	92	50/ Phase	0-1

Table 4.2 DERs Rating and Location

Number	**DER Type**	**Rating (kW)**	**Location (node)**
DER -1	Non-Renewable	45	250
DER -2	Non-Renewable	60	60
DER -3	Renewable (wind)	150	95
DER -4	Renewable (wind)	90	151

The hourly load demand profile for an entire year has been taken from [134]. The probability of occurrence of percentage of load demand with respect to peak load demand and cumulative probability of the load demand throughout the year have been shown in Figure 4.8. The fully loaded (100% load) condition is considered as a peak load demand. The wind power output throughout the year during different loading hours has been shown in box plot Figure 4.9.

4.6.2 Simulations and Results Discussion

The communication system is working well, and its delay effect has not been considered during the execution of CVR operation. The performance of proposed method has been

studied for two scenarios under following three different cases of VVC operation on the above-mentioned test system.

Table-4.3. Ratings and Parameters of CES system

Location/ Phase	Node-65/1
Rate kW power (P_{CES}^{rated})	50 kW
Rate kVAr power (Q_{CES}^{rated})	40 kVAr
Rated kWh capacity (kWh_{CES}^{rated})	150 kWh
Reserve kWh capacity ($kWh_{CES}^{\min}$)	20%
CES maximum voltage limit ($V_{CES}^{\max}$)	1.1 p.u.
CES minimum voltage limit ($V_{CES}^{\min}$)	0.9 p.u.
Inverter rating ($S_{CES,inv}$)	100 kVA
SOC range (SOC^{upper} - SOC^{lower})	90% - 20%
Inverter efficiency (η_{inv})	97%
Battery discharge efficiency (η_D)	94%
Battery charge efficiency (η_C)	97%
Charging/ discharging power factor	1/0.85

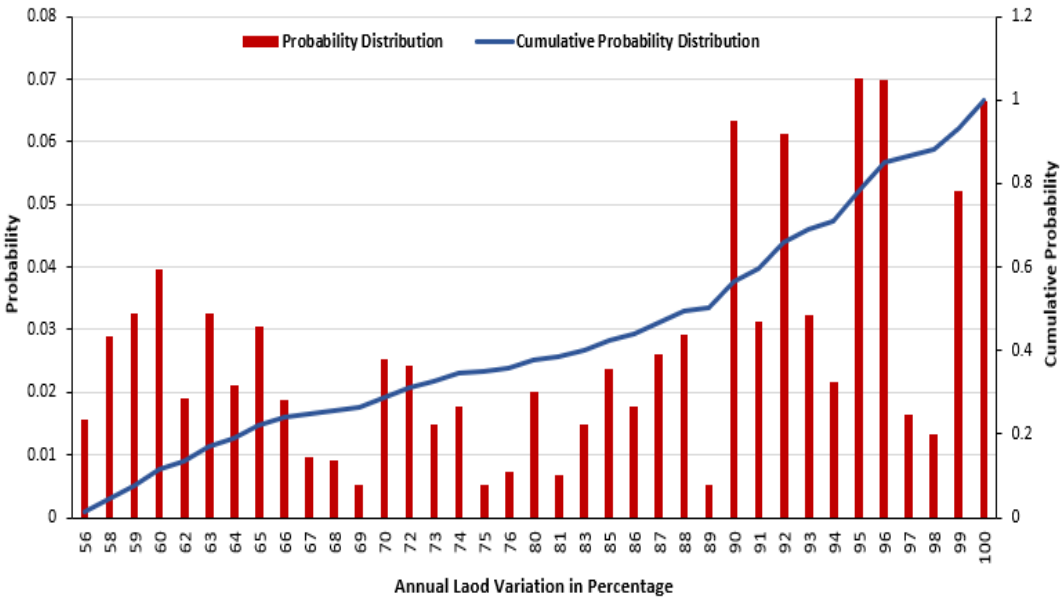

Figure 4.8 Annual load variation in percentage

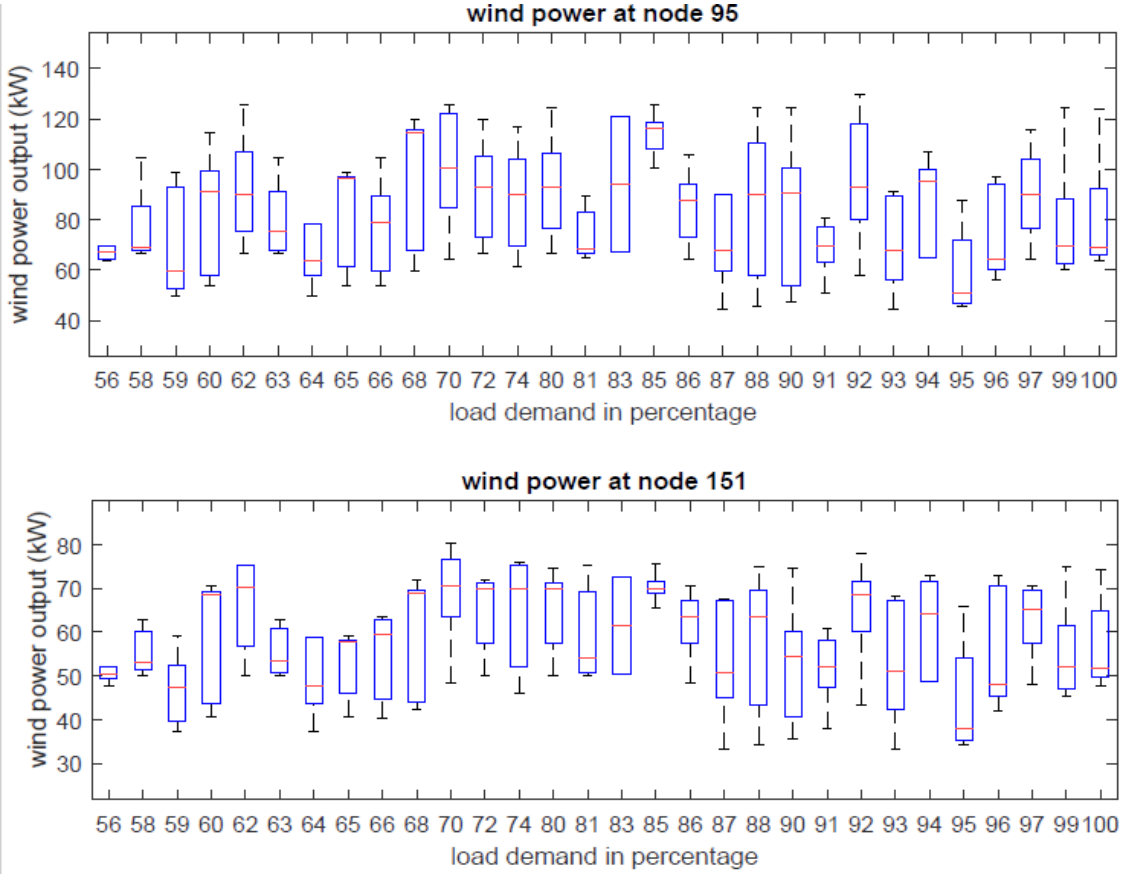

Figure 4.9 Wind power generation at node 95 and node 151 with varying load demand annually

(i) Case 1: Without CVR (Normal Operation)

In this case, the system does not deploy CVR or CES during VVC operation. The execution of VVC has been carried out at 120V regulated voltage with OLTC, AVR-1, AVR-2 and AVR-3 at 124 V. CBs are fixed in nature. The effect of CES has not been included in this case.

(ii) Case 2: With CVR only

In this case, VVC operation has been carried out CVR only taking in two subcases as discussed below.

- *Subcase I- Traditional CVR:* In present implementation of traditional method, the regulation voltage of 118V has been adopted for OLTC, AVR-1, AVR-2 andAVR-3 for enabling CVR. The level of voltage reduction can be increased by controlling the above

devices to achieve higher energy savings. However, continued reduction may lead to violation the minimum voltage limits at some points of the distribution network.

- *Subcase II- VVO based CVR*: The SG enabled CVR has been implemented through optimal VVC operation. The optimal operation has been carried out using proposed VVO method. In this case, impact of CES is not included.

(iii) Case 3: CVR with CES

In this case, the CVR is deployed along with CES device. The CVR is enabled through proposed method considering the presence of CES in the system. The allocation of CES system is based on the minimum node voltage. In this study, minimum voltage was observed at nodes 65 in phase A during normal operation. Therefore, CES unit was placed at node 65. Charging, discharging and power flow of CES have been controlled by proposed scheme as discussed earlier subsection.

4.6.2.1 Scenario-1: Demand reduction during fully loading hours

To evaluate the impact of CVR for peak demand reduction, the simulation has been carried out for above mentioned three cases of the system during fully loading hours of a typical year. Figure 4.10 shows the distributions of peak load hours throughout the year. It can be seen from the figure that peak loading occurs from 11th to 21st hours (excluding 13th; 16th and 17th hour) in daily operation.

- *Case 1:* The simulation results in terms of energy demand and losses, in this case, are shown in the second column of Table 4.4. The aggregated maximum and minimum load node voltage were 1.0451 p.u at node 82A and 0.9751 p.u. at node 65A respectively.
- *Case 2:* In this case, the test system has been simulated for CVR only with two subcases. The simulated results are depicted in Table 4.4. From results, it can be observed that CVR operation with VVO produced about 40.285 MWh, i.e. 2.19 % reduction in energy demand during fully loaded hours annually. Moreover, the reported energy

savings are higher than the traditional CVR method with slightly reduced energy losses. The calculated values of CVR_f are 0.592 and 0.811 for traditional and VVO based CVR respectively. From the simulated results, it is observed that VVO based CVR operation is a better choice for higher peak shavings and CVR factor with proper voltage regulation.

Case 3: The deployment of only CVR operation results in higher energy losses. In order to further reduce the energy losses and achieve higher peak shaving, the VVC operation has been carried out in VVO association with CES. The discharging and power flow controls have been adopted. The CES injects the active and reactive power to phase A in the present case. The simulation results obtained are shown in Table 4.4. The total energy savings of about 67.42 MWh, i.e. 3.0%, have been achieved. The maximum and minimum load node voltages are 1.015 p.u at node 1_B and 0.9532 p.u. at node 104_C respectively. Maximum energy demand reduction is reported in phase A, followed by phase C. About 2.07 % reduction in energy losses with respect to Case 1 has reported in this case. Moreover, the reported losses are lesser than Case 1 and Case 2.

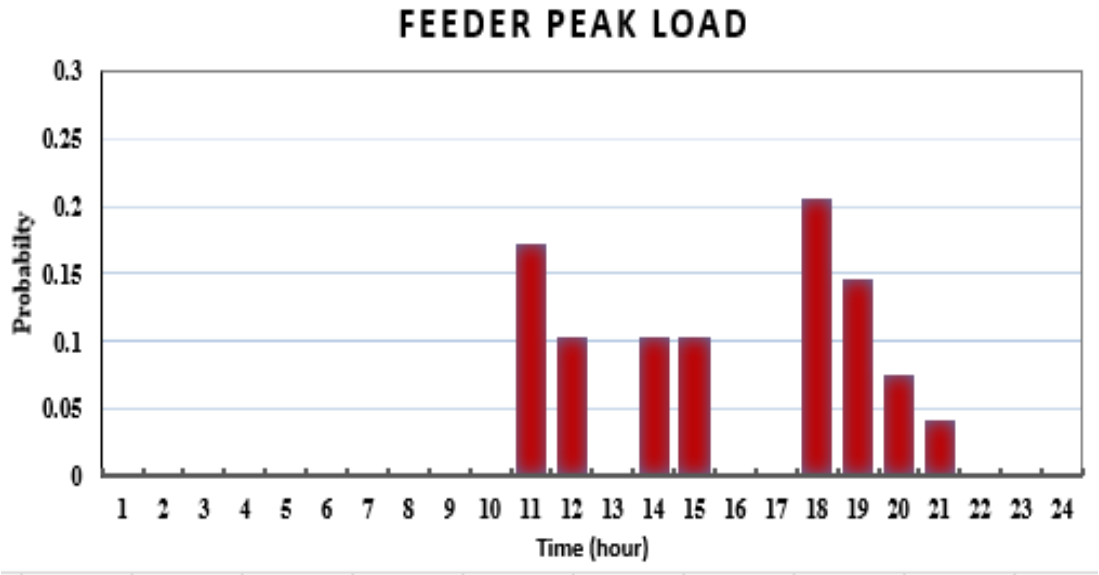

Figure 4.10 Distributions of peak load hours throughout the year.

Table 4.4 Simulation results for scenerio 1

Energy Terms		Case-1 (without CVR)	Case-2 (With CVR Only)		Case-3 (CVR with CES)	MWh Energy Change, (E_{Saving} in %)		
						Case-2		Case-3
			Traditional CVR	VVO based CVR		Traditional CVR	VVO based CVR	
Energy Demand	**Phase A**	852.385	832.922	832.922	805.673	14.0601	19.464	46.712
	Phase B	559.213	548.871	548.871	549.336	8.7155	10.342	9.877
	Phase C	691.158	674.948	674.948	674.657	11.0975	16.21	16.50
	Total	2102.76	2056.74	2056.74	2029.67	33.8771 (+1.611)	46.015 (+2.19%)	73.09 (+3.55%)
Energy Losses (MWh)		56.1827	56.357	57.7514	55.195	-0.1743 (0.31%)	-1.569 (-2.79%)	+0.9877 (+1.79%)
CVR_f		-----	0.592	0.811	0.82	-----	----	

4.6.2.2 Comparative analysis

A comparative study of proposed VVO method and MILP based VVO [12] has been analyzed for peak demand hour in the absence of CES and distributed generation. The simulation results are depicted in Table 4.5. It can be observed from the table that the proposed method yields higher reduction in system losses and power demand at the substation. In addition, the comparison of proposed DGSA and other heuristic optimization-based GA has also been carried out in the absence of DER. The simulations have been performed twenty-five times for both the method. Table 4.6 shows the result of both the methods for Case-2 and Case-3 with respect to the fitness value, standard deviation (STD), convergence (iteration) and CPU time. Figure 4.11 shows the convergence characteristics of both the optimization methods for both cases.

Table 4.5 Simulation results during peak load demand hour

Energy Term/devices		**MILP based VVO** [66]	**Proposed DGSA based VVO**
OLTC taps		[-1]	[+3]
AVR Tap	**AVR-1** **AVR-2** **AVR-3**	Fixed tap ratio (1:1)	[-5] [0, 0] [2, -3, -2]
Cap. steps	**CB-1** **CB-2** **CB-3, CB-4**	[2, 0, 1] [1] [0], [0]	[2, 2, 2] [1] [1], [1]
Losses (kW)		140.4	99.4
Min voltage elsewhere than slack bus		0.9505 p.u (at 66_C)	0.9520 p.u (at 114_A)
Max voltage elsewhere than slack bus (node)		1.0140 p.u. (at 149_B)	1.0188 p.u. (at 149_B)
Total active load (MW)		3.447	3.440
Total reactive load (MVAr)		1.873	1.6123
Active power at slack bus (MW)		3.588	3.540
Reactive power at slack bus (MVAR)		2.026	1.612
Phase wise (A, B, C) power factor at slack bus		0.91, 0.82, 0.87	0.907, 0.90, 0.92

Table 4.6 Comparative analysis of optimization methods

Measuring Parameters		Case-2 (CVR with VVO)		Case-3 (CVR with CES)	
		GA	DGSA	GA	DGSA
Fitness value (kW)	Best	3546.15	3540	3498.61	3493.42
	mean	3556.16	3546.8	3503.71	3497.93
	worst	3563.87	3550.8	3511.78	3505.2
Standard deviation (STD)		6.4949	3.3547	5.14220	4.3643
Required Iter for convergence		48	28	76	27
mean CPU time		216.61	120.05	217.761	120.27

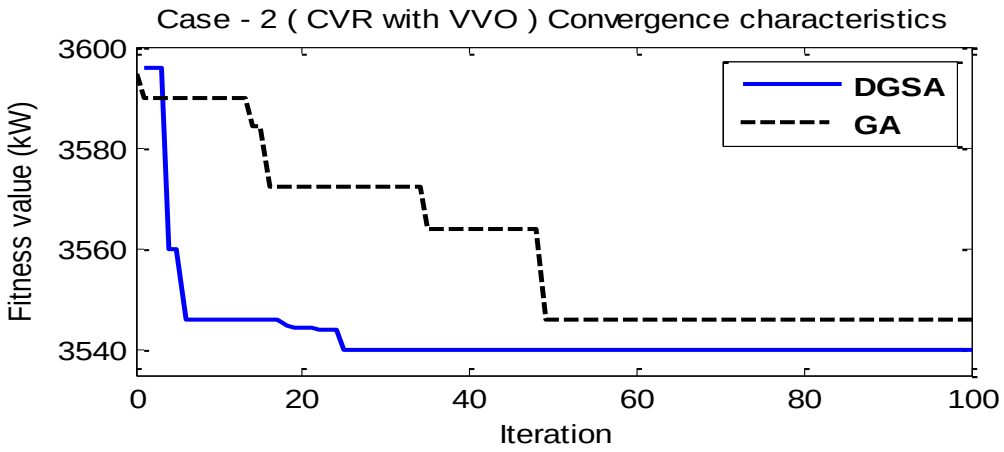

(a)

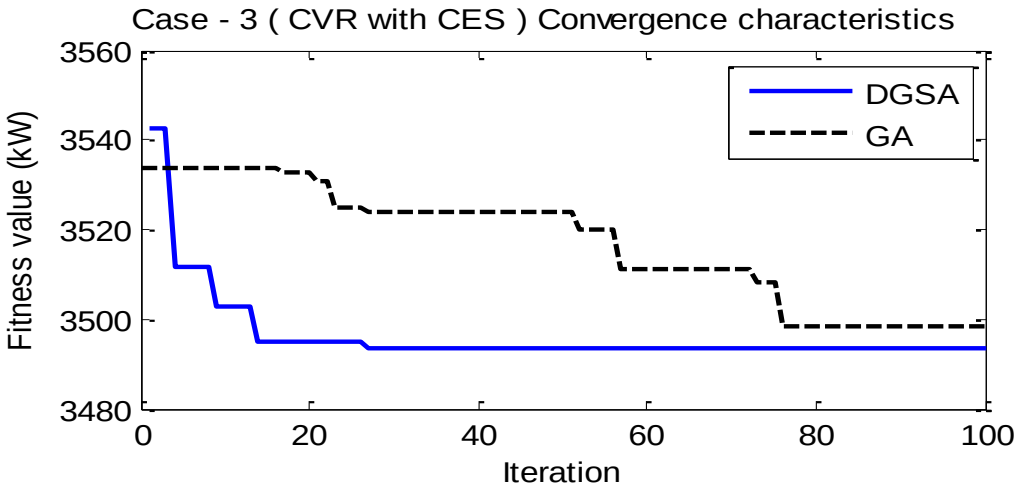

Figure 4.11 Iteration wise convergence characteristics for (a) Case-2 (VVO with CVR) (b) Case-3 (CVR with CES)

It can be observed from the figure and the table that the DGSA method has faster convergence with less computation time. The parameter of DGSA and GA used in this study are depicted in Appendix A, Table A.1.

4.6.2.3 Scenario-2: Energy saving and demand management during varying load hours

To estimate the energy savings and manage the demand through CVR alone and association with CES system, the test system has been simulated for the three cases discussed earlier with different load demand hours for the entire year. The varying load demands with a probability of occurrences have been shown in Figure 4.8 for the entire year. The wind DER power profile for the entire year during different loading has been shown in Figure 4.9. In this study, low loading situation is considered below 67% and high loading is above 94% of peak load demand. The simulated results of each case are discussed as under:

- *Case 1:* The simulation results for this case are depicted in Table 4.7. The aggregated energy demand and energy losses are shown in the second column of Table 4.7. The lowest voltage profile with different percentages of peak load demand for the entire year is shown in Figure 4.12 and it varies from 0.968 p.u. to 0.9978 p.u.
- *Case **2:*** The test system has been simulated for CVR only with the proposed VVO method and obtained results are shown in Table 4.7. From results, it can be observed that in the case of VVO based CVR only, significant aggregated energy savings of about 511.487 MWh, i.e. 2.297%, is achieved annually. Estimated energy savings directly reflect the reduction in energy demand and energy losses at the substation. The calculated aggregated value of CV Rf is 0.795 annually in this case. The lowest voltage profile with different percentages of peak load demand for the entire year is shown in box plot Figure 4.12 in case 2 and it can observe that voltage is above the minimum permissible limit

(0.95p.u.). Figure 4.13 box plot represents the achieved energy savings with respect to load demand and wind DER power output variation for the entire year.

- *Case 3:* In order to manage the peak load management and demand balancing, VVC has been carried out combined with CVR and CES using proposed VVO method. According to the CES power flow control strategy, as depicted in subsection *4.3.3*, node 65, phase A has highest, and phase B has lowest load demand. Therefore, during the discharging state, the CES system is connected in phase A and during the charging state, it is connected to phase B. Generated results are tabulated in Table 4.7. It can be observed from Table 4.7 that aggregated maximum demand reduction of 543.725 MWh is achieved with reduced energy losses. The lowest voltage profile with different percentages of peak load demand for the entire year is shown in box plot Figure 4.12 in case 2, and it can observe that voltage is above the minimum permissible limit (0.95p.u.).

  The CES active and reactive power profile has been shown in Figure 4.13 which indicates that during charging state CES operates on unity power factor consuming the active power of 50 kW. However, during discharging state CES operates with 0.85 power factor feeding 45 kW active power and 27.88 kVAR reactive power into the system. From Figure 4.14, it can be observed that lowest voltage variation in Case 1 is about 2% throughout the entire year. However, Case 2 and Case 3 have approx. 0.6 % voltage variation Figure 4.14 box plot (case 3) represents the achieved energy savings with respect to load demand and wind DER power output variation for the entire year.

Table 4.7 Simulation results for scenario 2

Energy Terms		**Case-1**	**Case-2**	**Case-3**	**MWh Energy/Current Change, (%E_{Saving})**	
		Without CVR	**With CVR (VVO based CVR)**	**CVR With CES**	**Case-2 (VVO based CVR)**	**Case-3 (CVR with CES)**
Energy Demand (MWh)	**Phase A (Φ_A)**	10582.98	10418.4	10302.19	164.58	280.79
	Phase B (Φ_B)	6969.09	6860.774	6963.94	108.316	5.148
	Phase C (Φ_C)	8575.022	8439.938	8439.57	135.084	135.452
	Total	26127.1	25719.1	25705.67	407.98 (+1.56%)	421.39 (+1.61%)
Energy Losses (MWh)		56.1827	603.41	618.39	14.975 (0.057%)	14.975 (0.057%)
CVR factor (CVR_f)		-----	0.637	0.667	--	--
Neutral currents during (A)	**Highest Load (100%)**	180.54 A	174.65 A	156.52 A	5.89A	24.02A
	Lowest Load (56%)	98.317 A	84.215 A	68.39 A	14.10A	29.74A

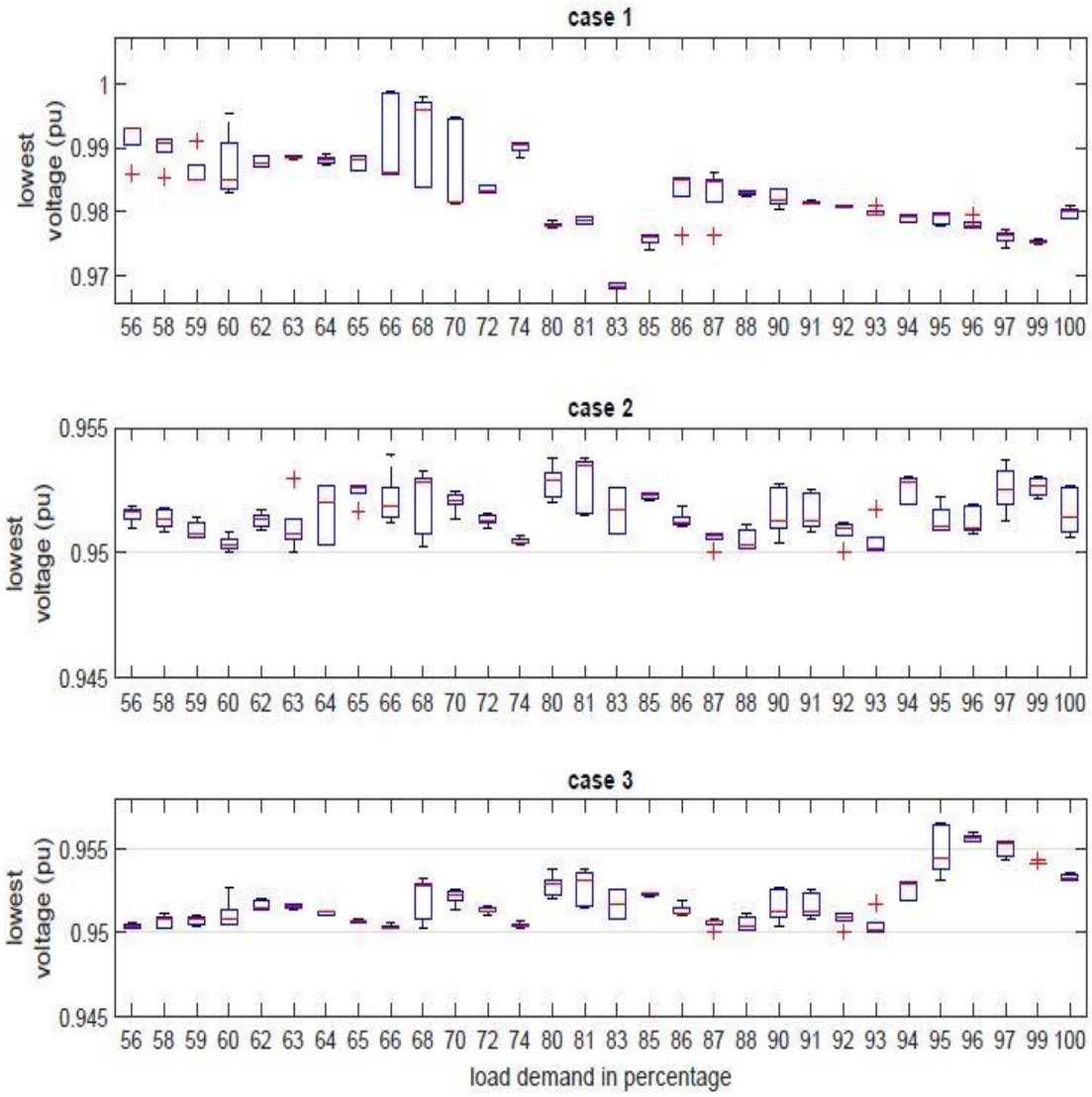

Figure 4.12: Feeder lowest voltage profile in different cases with varying load demand annually (a) *Case 1* (without CVR) (b) *Case 2* (with VVO based CVR) (c) *Case 3* (CVR with CES)

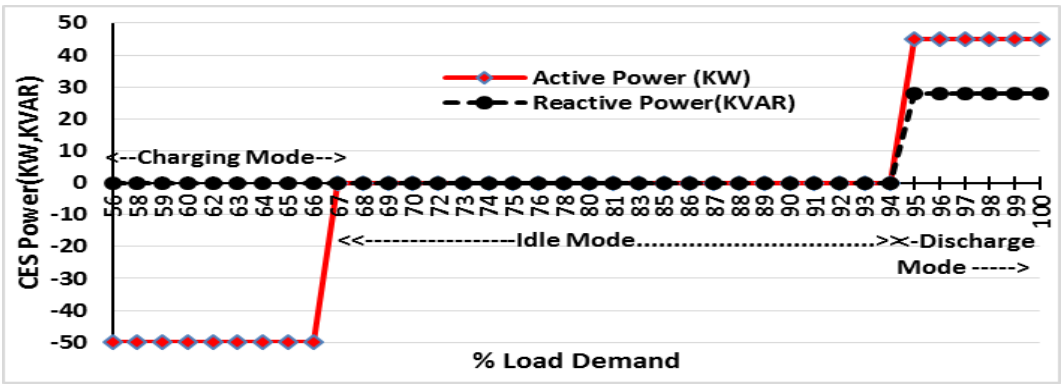

Figure 4.14: CES Active and reactive power profile

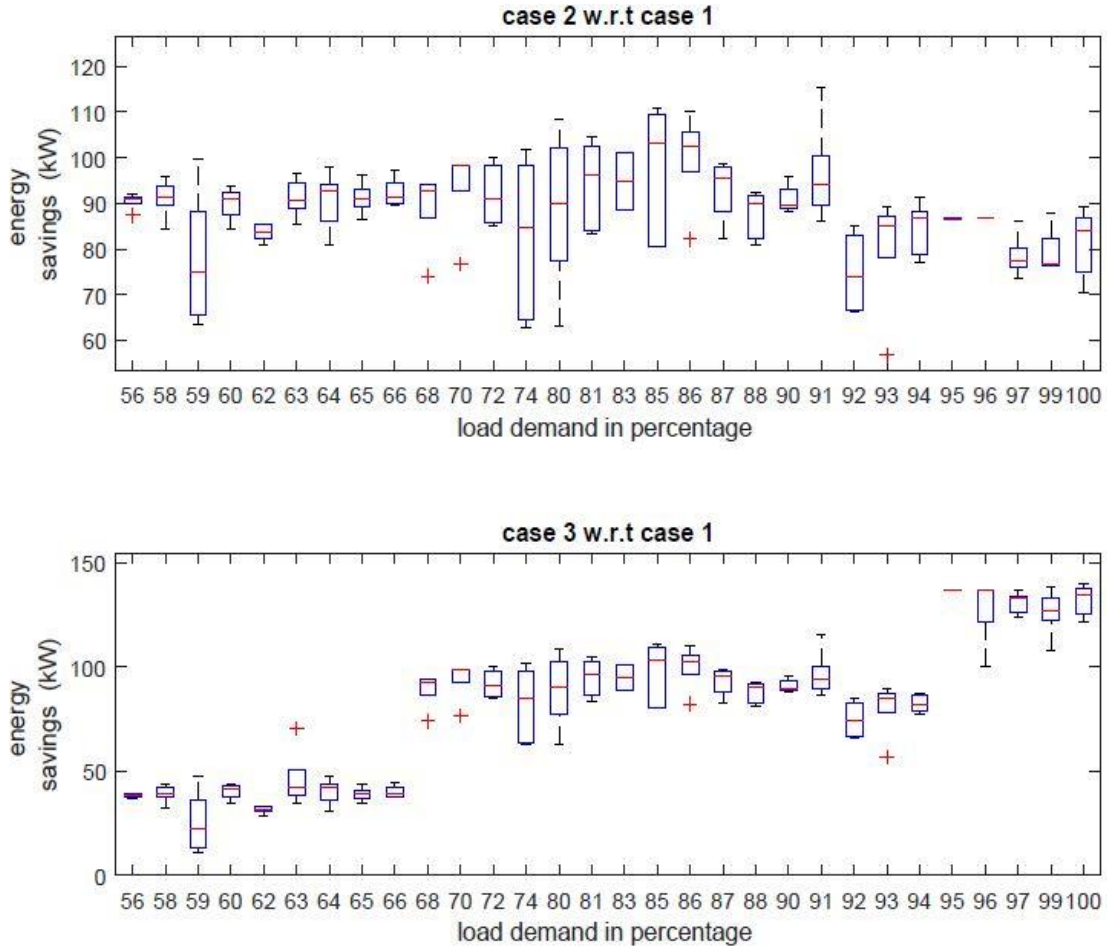

Figure 4.14: Energy savings (kWh) in *Case 2* and *Case 3* with varying load demand annually

4.6.2.4 Demand Balancing

Unbalance loading and imbalanced configuration produces operational issues such as the rise in neutral current and voltage in the distribution system. From the simulation results of Table 4.7, it can be observed that total energy demand is 26127.1 MWh and 25719.1 MWh for Case 1 and 2, respectively. In this, the share of phases A, B, and C are 40.5%, 26.67%, and 32.82%, respectively in both cases. However, in Case 3, the total energy demand shared by phases A, B and C are 40.0%, 27.09% and 32.83%, respectively. Moreover, in this case, there is a slight decrease in demand share of phase A and an increase in demand share of phase B in comparison to Case 1&2. The incremental change in demand share lead towards demand balancing. To elaborate further, the effect on

neutral current has been analyzed with VVO and CES. The magnitude of neutral currents at feeder head transformer during highest and lowest loading has been shown in Table 4.7 and it can be observed that higher reduction in neutral current has been produced with the application of both CVR and CES in comparison to Case1 and Case 2 in both loading scenarios. The decrease in neutral current assists in demand balancing. Hence, it can be concluded that the deployment of CES in association with the VVO engine is a helpful method for mitigation of rise in neutral currents.

4.6.3 Techno-economic Assessment

The performance of CVR scheme is assessed through energy, cost savings and CVR factors. The power and energy savings have been calculated using equations (4.1)- (4.2) for Case 2 and Case 3 operations. For cost savings estimation, equations (4.3) – (4.6) is directly applicable in Case 2 (only CVR) operation. However, cost-saving estimation during Case 3 (CVR with CES), the effect of CES operating and maintenance costs (C_{OMC}^{CES}) also be included in the cost function. The C_{OMC}^{CES} is further divided into two parts as first is the annual fixed CES operating and maintenance costs ($C_{OMC,Fixed}^{CES}$) and second is variable operation and maintenance cost ($C_{OMC,Var}^{CES}$) as defined in the below equations (4.36) and (4.37).

$$C_{OMC}^{CES} = C_{OMC,Fixed}^{CES} + C_{OMC,var}^{CES} \quad (4.36)$$

$$C_{OMC,Fixed}^{CES} = C1 \times Pces \quad (4.37)$$

$$C_{OMC,var}^{CES} = C2 \times \sum_t^T P_{Disch}^{CES}(t) \quad (4.38)$$

After adding the CES operating and maintenance cost the equation (4.6) can be rewritten as equation (4.39),

$$C_{cost}^{CVR\ with\ CES} = \sum_t^T [C_{Grid}(t) P_{demand}^{CVR}(t)] + C_{OMC,Fixed}^{CES} + C_{OMC,Var}^{CES} \quad (4.39)$$

The grid electricity (C_{Grid}) is dynamic changing throughout the year. For simplification, the annual grid electricity price has been split in three range first is 0.02$/KWh for load

demand up-to 75% loading, the second range is considered from 76 % to 94 % and electricity price is 0.3$/KWh. For the third range, i.e., from 94% to 100% load demand, the considered grid electricity price is 0.4$/KWh.

From Table 4.8, it can be observed that the cost savings achieved is about 1.67 % to 1.98 % annually with the deployment of CVR in Case-2(VVO based CVR) and Case-3 respectively. In Case-3, the achieved energy cost savings are much higher than the traditional CVR (LDC based method) and/or VVO based CVR and it can be clearly seen from Table 4.8 in both forms in terms of K$ and percentage. The economic CVR factor (K$) also higher in Case -3 in comparison to Case 2. Table 4.8 results also indicate that reduction in demand cost will directly result in under revenue collection temporarily for a utility point of view. However, this can be rectified later with suitable regulatory schemes such as revenue decoupling mechanism, which recovers revenue shortfall including any inevitable interest. The impact of CVR and CES technology on carbon emission has been studied. The emission rate and emission price have been taken as 0.4 tCo2e/MWh and $6.84/tCo2e, respectively. Table 4.9 shows the carbon emissions of the system in different cases. It can be observed that carbon emissions are reduced by amount 204.59 tCo2e and 217.49 tCo2e in case 2 and case 3 respectively. This is due to the maximum reduction of energy demand.

Table 4.8: Annual cost savings and economic CVR factor in both Case-2 and Case-3

Annual Cost Saving	**With CVR Only (Case -2)**		**CVR with CES (Case-3)**
	Traditional CVR	**VVO Based CVR**	
Saving in K$/year	96.534	134.9263	161.2716
Saving in percentage (%/year)	1.2	1.677228	1.98506
CVR factor in K$	0.491	0.67	0.807

Table 4.9: Annual environmental benefit in Case-2 and Case-3

Parameters	**Case1 (without CVR)**	**Case -2 (With VVO based CVR)**	**Case -3 (CVR with CES)**
Total demand (MWh)	22269.82	21758.33	21726.09
Co2 Emission (tCo2e)	8907.927	8703.332	8690.437
Reduction in Co2 emission (tCo2e)		204.59	217.49
Emission cost ($)	60930.22	59530.79	217.49
Savings in emission cost ($)		1399.428	1487.632

4.7 Conclusion

The VVO is a well-established method for improvement in the operation of distribution networks. The proliferation of CES has paved the way for achieving not only improvement in the system performance but also a reduction in peak load and demand balancing in addition. In order to utilize its benefits in CVR, VVO in association with CES approach has been implemented in this chapter. The investigation reported in present chapter focuses on the combined effect of CVR and CES on smart grid operation. The problem has been expressed as a Volt/VAR optimization problem, which minimizes the total power consumption while meeting the system constraints. The resulting optimization problem has been solved using DGSA driven VVO approach. The proposed methodology is capable of offering optimal coordination of VVO devices and VVO in association with CES in the presence of DER. The case studies on the modified 123 bus unbalanced system demonstrated that the proposed method effectively handled the VVO problem. The obtained results indicate that higher peak shaving, energy efficiency, peak load management, and reduced system losses are achieved when both CVR and CES are applied as compared to only CVR deployment. Besides, the cost-benefit analysis

authenticates the findings. Therefore, utility, prosumers and consumers would be benefitted under combined operation of VVO and CES for CVR technology.

Though the proposed single centralized VVO works well for fixed time step and constant power generation sources, but it lacks coordination with VVC devices under a sudden change in network behaviours such as variable power outputs from renewable DERs due to cloud transients' and other reasons. In this regard, next *chapter 5* presents a multi-stage multi-objective VVO methodology that takes care of both centralized as well as local VVC controls.